switching speed is 2 ms. A detailed examination of the phase of the output carrier would determine a lower bound on data rate in this mode.

## VI. Conclusions

It has been shown that the technique of mixing chirp signals produced by impulsing SAW filters enables FFH generation over a wide bandwidth with large numbers of selectable hop frequencies in simple, compact, low power hardware and provides a new capability in this area. The effects of imperfections in the SAW chirp filters on FH modem performance and CW generation have been discussed and it has been shown that although low spurious CW performance is beyond the current state of the art, low error-rate FFH modem operation is possible with available device designs.

In addition, a simple tracking filter module has been described which is capable of giving low spurious (−60 dBc) CW signals with acceptable switching speed. This module allows operation on fixed or slow hopping carriers in addition to the FFH capability. The combination of the two modules is not intended to compete with established synthesizer techniques for applications involving only slow FH.

## Acknowledgment

The authors gratefully acknowledge the contributions made by several colleagues, notably by J. C. Reid of the Wolfson Microelectronics Institute for experimental work on the tracking filter, R. A. Bale and C. T. Eustace of RSRE for experimental work on the FH generator, and R. Jenkins of MAv for implementation of data demodulator and tracking loop control circuits. The SAW filters were designed and produced by RACAL-MESL.

## References

[1] R. C. Dixon, *Spread Spectrum Systems*. New York, Wiley, 1976.
[2] C. Atzeni, G. Manes, and L. Masotti, "Programmable signal processing by analogue chirp-transformation using SAW devices," in *1975 IEEE Ultrasonics Symp. Proc.*, IEEE Cat. 75CH0994-4SU, pp. 371–376.
[3] P. M. Grant, D. P. Morgan, and J. H. Collins, "Generation and correlation of digitally controlled coherent frequency-hopped waveforms using surface acoustic wave devices," *Proc. IEEE*, vol. 64, pp. 826–828, May 1976.
[4] J. M. Hannah, P. M. Grant, and J. H. Collins, "Fast coherent frequency hopped waveform synthesis using SAW devices," in *1976 IEEE Ultrasonics Symp. Proc.*, IEEE Cat. 76 CHI 120-5SU, pp. 428–431.
[5] B. J. Darby *et al.*, "Performance of frequency hop synthesizers based on chirp mixing," in *1977 IEEE Ultrasonics Symp. Proc.*, IEEE Cat. 77 CHI 1264-1SU, pp. 514–523.

# Acoustoelectric Convolver Technology for Spread-Spectrum Communications

STANLEY A. REIBLE, MEMBER, IEEE

*Abstract*—**Acoustoelectric (AE) convolvers for spread-spectrum communication applications are described with input bandwidth capacities to 200 MHz. These devices offer an unique combination of large processing gain, high dynamic range, small size and weight, and low drive power requirements. The programmable feature of convolvers allows the encoding waveform to be changed from bit-to-bit, thereby providing resistance to repeat jamming and enabling secure communications.**

**The basic concepts of a convolver-based spread-spectrum communications system are reviewed, current convolver capabilities are discussed, and projections are made for future device performance. Deviations from nonideal convolver performance are considered. Special techniques which must be used in the system implementation and evaluation of convolvers are described, and the performance level achieved in a state-of-art convolver subsystem is given.**

Manuscript received April 15, 1980; revised October 13, 1980. This work was supported by the Defense Advanced Research Projects Agency and the Department of the Army.

The author is with Lincoln Laboratory, Massachusetts Institute of Technology, Lexington, MA 02173.

## I. Introduction

THE convolver [1] can function as a programmable matched filter for wide-band spread-spectrum waveforms. The programmable feature of convolvers allows the encoding waveform to be changed from bit-to-bit, thereby providing resistance to repeat jamming and enabling secure communications. Since the matched filter function is determined electronically in a convolver, this device does not suffer from the temperature related phase problem of a conventional surface-acoustic-wave (SAW) matched filter with a comparable time-bandwidth product. A dual convolver [2] provides a convenient method of demodulating

0018-9480/81/0500-0463$00.75 ©1981 IEEE

differential-phase-shift-keyed (DPSK) data. A SAW filter [3] provides a method of generating wide-band minimum-shift-keyed (MSK) signals for convolver-based systems. A convolver-based system can provide fast synchronization [4] and low probability of intercept (LPI).

The functioning of analog convolvers depends upon three basic operations; delay, multiplication (or mixing), and integration. The three competitive types of convolvers which currently exist are the 1) acoustoelectric (AE) [5], 2) elastic [6], and 3) acoustooptic [7] devices. All three devices depend upon acoustic lines for delay. For mixing, the AE device utilizes the strong nonlinearities of a bulk semiconductor, typically silicon, coupled through an intervening air gap to the piezoelectric delay line or upon a semiconductor film which has been deposited directly on the piezoelectric substrate. An alternative approach is to deposit a piezoelectric film, typically zinc oxide, on a bulk semiconductor [8]. Elastic convolvers utilize the weak nonlinearity of the piezoelectric substrate, typically lithium niobate, and usually depend upon some form of acoustic beam compression to increase device efficiency. For mixing, acoustooptic convolvers employ double diffraction of incident light by the propagating surface acoustic waves or square-law operation of a photo detector. For integration, AE devices utilize a conducting contact along the back side of the semiconductor, elastic devices use a conducting strip directly on the piezoelectric substrate, while acoustooptic devices employ a lens to collect the diffracted light and focus it on a photodetector.

Gap-coupled AE convolvers [2], [9] with input bandwidths of 100 MHz exist as fully engineered devices, tolerant of mechanical shocks, and ready for use in fielded equipment. These devices provide a processing gain of 33 dB with a dynamic range exceeding 50 dB. Recently the input bandwidth of AE convolvers has been extended to 200 MHz [10]. A mechanical support structure has been developed which maintains a uniform air gap and ensures stable device operation over a 100°C temperature range [2]. These devices have passed stringent vibration tests for military aircraft, jeep, and tracked-vehicle radio equipment [10].

Monolithic AE convolvers are in the preliminary stages of development. In the past, these devices have had limited performance due to large acoustic propagation losses or excessive dispersion.

Elastic convolvers provide a low cost alternative to the AE device. Elastic convolvers have existed in a well-engineered form for about six years [12] but with moderate bandwidths ($\sim$50 MHz). More recently, the bandwidth of elastic convolvers has been extended to 100 MHz [13], [14]. Further development by several commercial firms is currently being pursued on these elastic devices. In the future the elastic convolver will probably dominate its AE cousin in most applications except those requiring the most extreme time-bandwidth products.

Acoustooptic convolvers have the potential of device bandwidths up to 500 MHz with maximum interaction lengths equal to that obtainable with AE devices ($\sim$50 $\mu$s) [15]. But these devices do not exist in a well-engineered form and integration into small packages has yet to be demonstrated.

This paper reviews the basic concepts and operation of a convolver-based subsystem first demonstrated at Lincoln Laboratory and currently under extended development at Texas Instruments, Inc. The achieved performance specifications for the convolver subsystem are given. Recent advances in gap-coupled AE convolver performance are discussed and the limits of device performance are projected. Throughout the paper, special attention is given to those convolver parameters (such as dynamic range, spurious signal levels, temperature effects and implementation loss) which are most critical in a system context. Deviations from nonideal convolver performance, as well as special techniques essential to system implementation and convolver evaluation are described.

## II. A Convolver Based Communication System

Convolvers can serve as the principle signal-processing component in a radio network designed to handle addressed packets of digital information [16]. The convolver can match filter the signal and demodulate the data. By using a convolver as a matched filter, the signal-to-noise ratio of the input signal is improved by a factor called the processing gain. The maximum potential processing gain of the convolver is equal to its time-bandwidth product, and in well-engineered integrations of convolver and peripheral electronics, this maximum processing gain can, to within about 1 dB, be realized.

To provide for protection against both intentional and unintentional interferences, it is desirable to employ a spread-spectrum technique which extends the signal bandwidth well beyond that necessary to transmit data at the chosen rate ($R$). One technique employs pseudonoise (PN) modulation to achieve bandwidth spreading. Such a system is shown schematically in Fig. 1. Here a PN generator produces a stream of binary "chips" at $nR$ chips per second, where $n$ is an integer several orders of magnitude larger than unity. During data transmission the output from the PN generator and a data buffer are combined in a modulo-two adder. At the start of each chip interval an impulse generator produces a positive or negative impulse, depending upon the output state of the modulo-two adder. This impulse is applied to an MSK SAW modulator which generates a phase-encoded waveform centered at the IF frequency $f_c$. The relative phase of the modulator output is shifted by $\pm\pi/2$ rad during the chip interval depending upon the sign of the impulse. The instantaneous frequency of the MSK modulator output over the chip interval is $f_c \pm nR/4$. The MSK spread-spectrum waveform has a null-to-null bandwidth 1.5 $nR$ [17]. The major advantage of MSK modulation is that it produces a more rapid falloff of frequency sidelobe energy than phase-shift-keyed (PSK) modulation. This lowers both cross-channel interference and potential loss in processing gain (implementation loss) due to received signal energy which falls outside the convolver passband. With this waveform the nominal processing gain is $10 \log n$ dB where $n$ is the number of chips per bit. The operation of the MSK modulator is discussed in

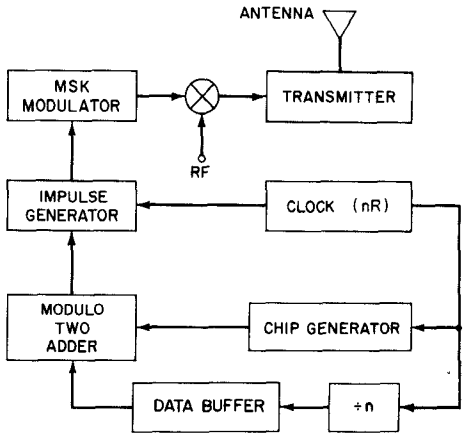


Fig. 1. Spread-spectrum waveform generator and transmitter.

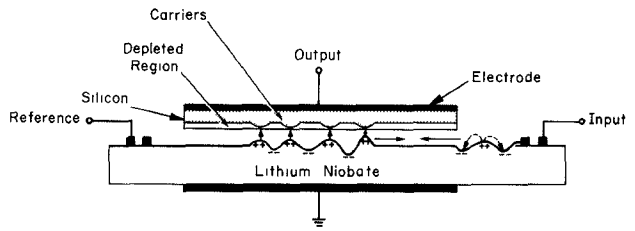


Fig. 2. AE convolver.

greater detail in a companion paper by Goll [18].

In the receiver the incoming signal is amplified, down converted to $f_c$ and applied to the convolver input port. To match filter the input signal it is necessary to generate a time-reversed replica of the transmitted chip code and introduce it into the reference port of the convolver. The operation of a convolver may be understood by referring to Fig. 2, which shows a piezoelectric substrate (typically lithium niobate) coupled across a gap of several hundred nanometers to a semiconductor (usually silicon). The input and reference signals are transduced to surface waves at opposite ends of the piezoelectric delay line. While these waves are under the semiconductor, their piezoelectric fields extend across the air gap, and mixing products are produced by the nonlinearity of the semiconductor. The local products are spatially integrated by the semiconductor. Propagation of the signals from opposite ends of the structure produces a relative reversal and shifting of the waveforms, while the semiconductor multiplies and integrates; thus the output can be seen to represent the convolution of the input signals. Because both of the spatial patterns are moving, there is a halving of the time scale at the output; that is, the center frequency and bandwidth are doubled. The output signal is given by

$$c(t)=K\int_{t-T}^{t} r\left(t-\frac{z}{v}\right)s\left(t-T+\frac{z}{v}\right)\frac{dz}{v} \qquad (1)$$

where $K$ is a scale factor, $r(t)$ and $s(t)$ are the reference and input signals, $v$ is the acoustic-wave velocity, and $T$ is the SAW transit time under the silicon. It can be seen from (1) that when $r(t)$ and $s(t)$ are properly timed and also of duration less than $T$, then the integrand is identically zero outside the limits of the integral, and hence $c(t)$ will be precisely the convolution (with the change in time scale and a delay, of course). Since convolution and correlation are related by a time reversal, a convolver serves as a programmable matched filter when $r(t)$ is a time-reversed replica of the desired waveform. Since the signal and reference counterpropagate along the same path within the convolver, they both undergo the same phase shift with temperature and material variations. Hence, the matched filtering function of AE convolvers is temperature insensitive. If the bandwidth-spreading waveform is changed from bit-to-bit, protection against repeat-jamming is obtained, as well as greater potential for secure communications.

For PSK (or MSK) encoded waveforms, data information is contained in the phase relationship between the bit energy and a local reference. For example a differential phase of 180° may correspond to a binary "1", while 0° corresponds to "0". Demodulating PSK-encoded data requires a phase comparison between the convolver output (the correlation spike) and a *coherent* local oscillator, which is unavailable in many communications systems. For DPSK-encoded waveforms standard PSK (or MSK) encoding is used for each bit but data information is contained in the differential phase relation between two adjacent bits. In this case no coherent reference is required, but two adjacent bits must be match-filtered, and their relative phases compared. At first glance this would appear to require an extremely stable delay line in order to allow phase comparison between adjacent bits. Separate acoustic delay lines and convolvers would not track exactly in delay, and phase problems with temperature would result.

Since a convolver has no phase problems with temper-

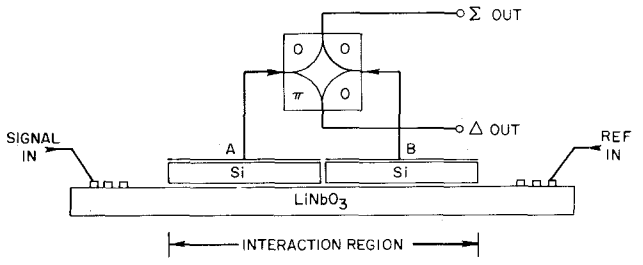


Fig. 3. DPSK convolver with hybrid.

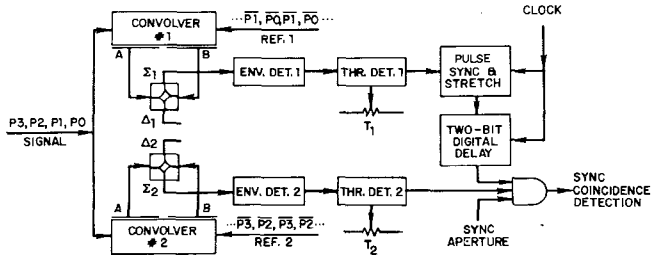


Fig. 5. Coincidence-detection block diagram.

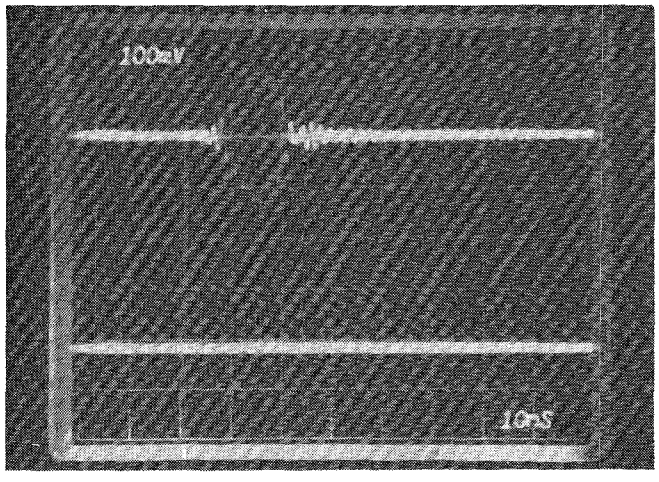


(a)

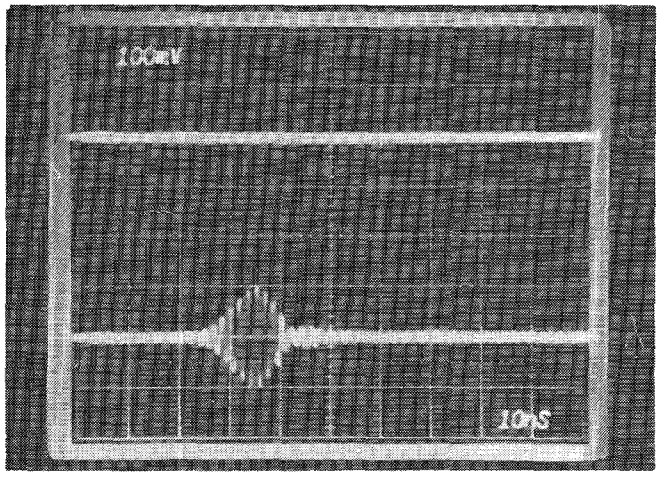


(b)

Fig. 4. Output from sum port (top trace) and difference port (bottom trace) of the convolver hybrid using a MSK encoded waveform for (a) no phase reversal, and (b) phase reversal between adjacent bits.

ature, it is appropriate to use a single device, but to segment the silicon into two equal elements, each 1 bit in length [2]. The two surface waves still share the same acoustic path, and now a phase comparison of the simultaneous correlation spikes of two adjacent bits can be performed in a sum–difference hybrid with inherent temperature stability. A DPSK convolver and its output hybrid are shown schematically in Fig. 3. The output of the convolver is shown in Fig. 4 when a) no phase reversal is present so that the output appears at the hybrid sum port, and b) with a phase reversal between adjacent bits so that the output appears at the difference port. The lack of crosstalk indicates good isolation and phase balance between the convolver outputs. Normally the bandwidth-spreading waveform is changed on every data bit by selecting successive 1000-bit binary codes from a very long sequence. When a single code is used repetitively, spurious sidelobes as high as $-14$ dB are observed. With a constantly changing input waveform, only a noise-like sidelobe level is observed having a measured rms level of approximately $-25$ dB.

To realize the full processing gain and dynamic range of the convolver it is essential to achieve proper alignment (synchronization) of the input and reference signals under the silicon. This is often the major problem in systems that employ a "burst" mode of transmission and the convolver does impose some practical limitations. Essentially, a higher output signal-to-noise is desired to achieve "sync" than to demodulate the data. A fast synchronization scheme for convolvers has been demonstrated [6]. In this convolver implementation, the transmitter generates a burst-format message consisting of a short 13-bit sync preamble followed by 1024 data bits. Every message bit (preamble and data) has a different PN spreading code. The exact code will have been previously agreed upon and will be valid for only a relatively short period of time (commonly called the code validity interval). After each period a new code becomes valid.

The receiver detects the presence of a message, aligns its reference code generator to the received preamble, and subsequently demodulates the data portion of the message. Since serial loading of a 2-bit dynamic reference takes 2 bit-times, the DPSK convolver can only perform a useful data bit demodulation once every 2-bit period. Therefore, for continuous DPSK data demodulation, the receiver requires two DPSK convolvers operating on data bit-pairs in bit-staggered fashion.

By employing a coincidence-detection concept, the receiver can take full advantage of the available pair of convolvers in processing the first four preamble bits ($P_0$–$P_3$). During initial message detection the first two reference bits ($\bar{P}_1$, $\bar{P}_0$) are recirculated in Convolver 1 while the third and fourth reference bits ($\bar{P}_3$, $\bar{P}_2$) are recirculated in Convolver 2 as indicated in Fig. 5. No data is present in the preamble bits. The sum output from Convolver 1 is envelope-detected, threshold detected, passed through a 2-bit digital delay and applied to a coincidence-detection gate.

The sum output from Convolver 2 is likewise envelope-detected and threshold detected, then applied to the coincidence-detection gate. When processed signals from both convolvers arrive simultaneously at the gate and a sync-aperature is enabled, a coarse-sync-coincidence detection is declared. Subsequently, during the fifth preamble bit, the reference is aligned to the input signal to an accuracy of about 1 chip interval. The reader will find further details on the synchronization procedure in [6].

## III. The DPSK Convolver

Gap-coupled AE convolvers [1], [2], [9]–[11], [18]–[21] have undergone extensive development during the past decade and now exist as an extremely useful circuit element. In this section the salient parameters of two DPSK convolvers developed at Lincoln Laboratory having input bandwidths of 100 and 200 MHz are reviewed. These devices are designed to operate over a temperature range of $-25°$ to $+75°C$ and have proven to be highly reliable over extended periods of operation.

The advertised temperature insensitivity of acoustoelectric devices is only available if a uniform, stable, submicron air gap can be maintained over a wide temperature range. This is achieved with the use of the mechanical structure shown in Fig. 6. Three spacer rails formed by ion beam milling the surface of the lithium niobate delay line, allow the silicon to rest firmly against the acoustic substrate. The silicon strips are bonded to a flexible polyimide sheet for easy handling and alignment during assembly. A second polyimide sheet contains the output connections and silicon termination resistors [19] or inductors [20]. Electrical connection to the silicon is made via plated-through holes on the polyimide sheets and pressure contact. The use of flexible circuitry allows a uniform pressure to be applied directly behind the silicon strip [2]. Thus beryllium–copper springs push on a thin diaphragm which, in turn, applies pressure to a jelly-like RTV rubber. This results in an essentially hydrostatic pressure against the polyimide sheet, and the characteristics of the springs and rubber are such as to maintain this pressure fairly constant over a wide temperature range.

Fig. 7 shows a convolver at a partially assembled stage. The 10-cm long $LiNbO_3$ delay line and two microstrip input-matching networks are mounted into an aluminum base. Two 3.5-cm long silicon strips are indium bonded end-to-end on a polyimide sheet. The convolver pressure-plate is seen with the second polyimide sheet in place. During the gap assembly procedure the delay line and silicon are given a final cleaning to remove any particulate contamination which could interfere with gap uniformity. The silicon is then aligned to the 0.78-mm wide acoustic path of the delay line to an accuracy of $\pm 0.02$ mm. After gap assembly, the convolver is hermetically sealed with indium gaskets. The size of the assembled device is 4.8 cm (wide) $\times$ 1.4 cm (high) $\times$ 12.1 cm (long) and it has a weight of 220 g.

There were two major design goals for the silicon support structure: 1) to obtain the desired device response; and

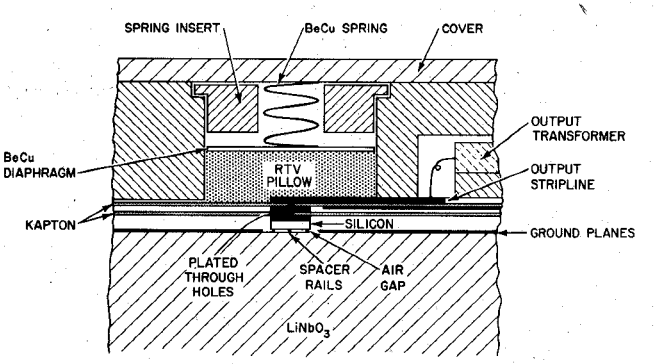


Fig. 6. Cross-sectional view of the convolver structure. Beryllium–copper springs act against a layer of RTV to apply a uniform pressure to the top of the silicon.

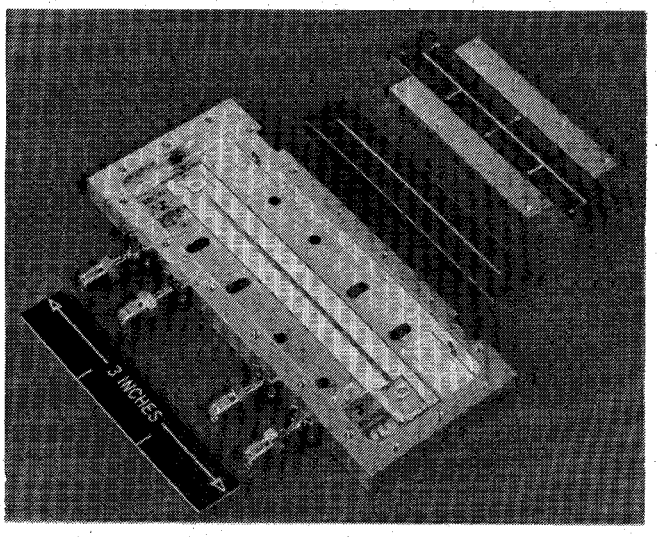


Fig. 7. The three principle DPSK convolver subassemblies; lithium niobate delay line in convolver base, silicon–polyimide sheet, and convolver pressure plate.

2) to stabilize the device by employing a structure which has minimal undesirable effects on the acoustic wave and yet is rigid enough to minimize deflection of the silicon. These goals have been achieved with a three-rail support structure [11]. Rail supports establish well-defined waveguide modes, which can propagate with minimal loss, but excitation of several modes by the incident acoustic beam can introduce amplitude ripple in the frequency response of the convolver. By maximizing the rail spacing and by carefully choosing the location of the rails in the acoustic-beam path, waveguide moding effects and scattering losses have been reduced to negligible levels ($<1$ dB).

In order to demonstrate the structural ruggedness of the gap-coupled convolver, a series of lengthy dynamic shock and vibration tests have been performed. The specifications of these tests are consistent with MIL-STD-810C for aircraft, jeep, and tracked-vehicle radio equipment. The dynamic tests consisted of 1) a CW vibration test, 2) a random vibration test, and 3) a shock test. These test specifications and data are summarized in Table I.

The input signals were PN-encoded with 1024 chips per 11-$\mu$s bit. The correlation peak of this PN code was moni-

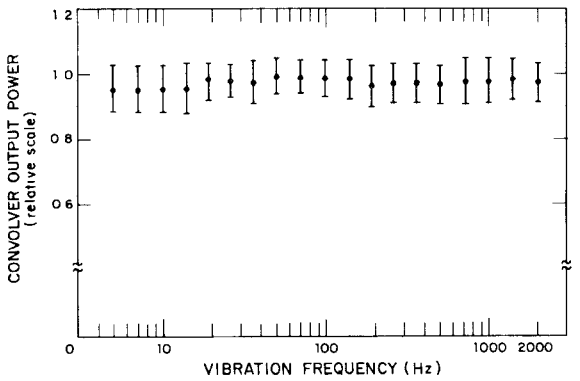


Fig. 8. Output response of a gap-coupled convolver with a interaction length of 22 $\mu$s when subjected to sinusoidal vibrations. Shown are the average output power and its standard deviation during the 9-h long CW vibration tests which included three frequency sweeps on each of the three axes.

TABLE I
VIBRATION TESTS OF DPSK ACOUSTOELECTRIC CONVOLVER

| | |
|---|---|
| (1) CW VIBRATION TESTS | |
| Vibration Frequency Range | 5 to 2000 Hz |
| Maximum Acceleration | 10 g |
| Time Duration | 3 hrs/axis, 3 axes |
| (2) RANDOM VIBRATION TESTS | |
| Vibration Frequency Range | 15 to 2000 Hz |
| RMS Acceleration | 16.4 g |
| Time Duration | 1 hr/axis, 3 axes |
| (3) SHOCK TESTS | |
| Maximum Acceleration | 40 g |
| Shock Time Duration | 11 msec |
| Number of Shocks | 6 shocks/axis, 3 axes |

*These tests are consistent with military standard for aircraft Jeep and tracked-vehicle equipment

tored at the convolver outputs throughout the tests. Fig. 8 is a plot of the convolver output power versus CW vibration test frequency. No serious degradation in performance of the convolver was observed during the dynamic tests. After the completion of the tests, the frequency response and interaction uniformity were measured and no degradation was observed.

A useful parameter for the convolver is its conversion efficiency, defined by

$$F = 10 \log \frac{P_o}{P_s P_r} \tag{2}$$

where $P_o$ is the output power and $P_s$ and $P_r$ are the signal and reference input powers, respectively. Knowledge of the conversion efficiency allows the output level to be calculated for arbitrary input signal levels. The term "conversion efficiency" is used in the same sense as for mixers and other parametric devices. The conversion efficiency scales approximately inversely with the time-bandwidth product of an acoustoelectric convolver.

TABLE II
ACOUSTOELECTRIC CONVOLVER DATA

| Center Frequency (MHz) | Bandwidth (MHz) | Interaction Length ($\mu$s) | Silicon Segments | F Theoretical (dBm) | F Measured (dBm) | Max Output Power (dBm) |
|---|---|---|---|---|---|---|
| 100 | 20 | 10 | 1 | -55 | -55 | -26 |
| 200 | 40 | 10 | 1 | -61 | -63 | - |
| 300 | 100 | 22 | 2 | -68 | -68 | -31 to -35 |
| 500 | 200 | 12 | 2 | -77 | -78 | -42 |
| 500 | 240 | 12 | 4 | -74 | -75 | -47 |

The $F$-factor for an AE convolver can be shown to be equal to [22]

$$F = \left(\frac{T^4}{W^2}\right)(M^2)\left(\frac{H^2}{2R_L}\right)(A) \tag{3}$$

where

- $T$ transducer electrical amplitude to acoustic amplitude transfer factor,
- $W$ acoustic beamwidth,
- $H$ output circuit voltage transfer function,
- $R_L$ load resistance,
- $A$ acoustic loss factor,
- $M$ internal efficiency factor.

The internal efficiency factor for an AE convolver is given approximately by

$$M = \frac{4\mu\alpha}{\omega v \epsilon} e^{-\alpha L} \tag{4}$$

where

- $\mu$ semiconductor mobility,
- $\alpha$ AE attenuation constant,
- $L$ device length,
- $\omega$ acoustic frequency in radians,
- $\epsilon$ semiconductor dielectric constant,
- $v$ SAW velocity.

A comparison of the theoretical and measured values of $F$ for silicon–lithium niobate (Si–$LiNbO_3$) gap-coupled AE convolvers is given in Table II. One sees agreement to within several decibels for a wide range of devices. The theoretical model should be valid up to center frequencies of several gigahertz.

The mechanical stability of the gap-coupled structure is more than adequate. Extensive temperature cycling experiments [2] indicate that the structure is also stable thermally, with the only temperature sensitivity due to the silicon itself. As indicated in (4), the conversion efficiency of the convolver is dependent upon the mobility of the charge carriers in the silicon. As the ambient temperature increases, carrier mobility decreases with a corresponding decrease in device efficiency. The theoretical internal efficiency factor of the 100-MHz bandwidth DPSK con-

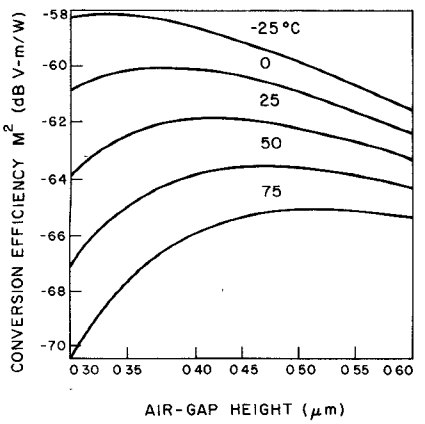


Fig. 9. Internal efficiency $M^2$ of DPSK convolvers with 30-Ω·cm silicon and a 22-$\mu$s interaction length as a function of air-gap spacing at several different temperatures.

TABLE III
DPSK CONVOLVER CHARACTERISTICS

| | | |
|---|---|---|
| Input Bandwidth | 100 MHz | 200 MHz |
| Interaction Length | 22 μsec | 12 μsec |
| Time-bandwidth Products | 2200 | 2400 |
| Input Center Frequency | 300 MHz | 500 MHz |
| Conversion Efficiency (F, to sum port) | -68 dBm | -78 dBm |
| Maximum Output Power | -34 dBm | -42 dBm |
| Dynamic Range (above KTB x N.F.) | > 57 dB | 46 dB |
| Interaction Uniformity | ± 1/2 dB | ± 1/2 dB |
| Input/Output Isolation | > 60 dB | > 60 dB |
| Isolation Between Output Ports | > 35 dB | > 35 dB |
| Input VSWR | < 3:1 | < 6:1 |
| Output VSWR | < 3:1 | < 4:1 |
| Spurious Signals | > 45 dB down | > 50 dB down |
| Acoustic Phase Distortion | ± 15° | ± 20° |
| EM Phase Distortion | ± 45° | ± 45° |

volver as a function of gap height is shown in Fig. 9. Multiple curves indicate the change in efficiency as the temperature is increased from −25° to 75°C. For devices having a gap height of 0.50 $\mu$m and 30-Ω·cm silicon, the predicted change in efficiency is about 5 dB. Increasing the gap height will reduce the temperature dependence of the device, but at the expense of reduced device efficiency. Since the output level of the convolver can vary with temperature it may be necessary to add additional circuitry which adjusts the threshold setting used during the detection of the synchronization pulses.

Table III lists the measured parameters for DPSK convolvers having center frequencies of 300 and 500 MHz and input bandwidths of 100 and 200 MHz, respectively. These parameters were obtained with gated CW inputs. The devices employ 2.5-finger-pair interdigital transducers having acoustic apertures (0.71 mm) of 62 and 102 wavelengths at 300 and 500 MHz, respectively. In order to obtain large fractional bandwidths, a quarter-wavelength

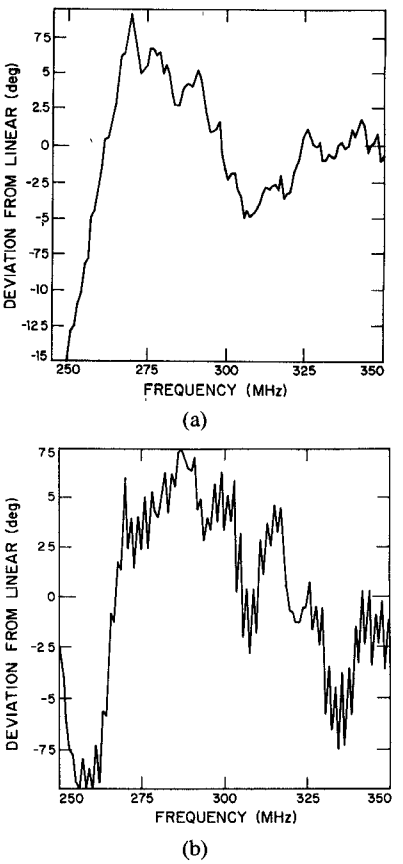


Fig. 10. Phase distortions in DPSK convolver: (a) acoustic delay line, and (b) output port.

inverter [23], a 4:1 impedance transformer, and a series tuning inductor are employed in the matching network of each transducer. A fractional bandwidth of 48 percent (240 MHz) has recently been obtained with a 500-MHz device [24]. Measured frequency response data on the DPSK convolvers is given in [10] and [11]. Since the output frequency of the convolver is twice the input frequency, it is relatively easy to suppress most spurious signals such as direct electromagnetic (EM) feedthrough to below the thermal noise floor with appropriate filters.

The device response must demonstrate a high degree of phase linearity in order to insure small implementation losses. Phase distortions of two types are significant in convolver structures, those which arise from the acoustic input line and the EM output line.

Acoustic distortions (deviation from best fit-to-linear) have been measured on several 100-MHz bandwidth convolvers with a pulsed phase bridge [25]. A frequency doubler was used as the reference for the output port characteristics. The measured delay line responses and the convolver output response, such as for the device shown in Fig. 10, indicate maximum acoustic phase distortions of ±15°. The dominant source of acoustic phase distortion appears to be the inductor-tuned transducers, the extraneous ripples are probably due to bulk acoustic waves or higher order waveguide modes. Delay line measurements on the 200-MHz bandwidth device indicate a maximum

acoustic phase distortion of $\pm 20°$ at the band edge. Convolver output distortions have not been measured on this device, but are expected to be of approximately the same magnitude as the delay line distortions.

The silicon in place on the $LiNbO_3$ forms a short microstrip line. EM phase distortions result from differences in propagation path length between local interaction points and the output tap on the silicon. The devices listed in Table III have silicon lengths which correspond to nearly one-half an electromagnetic wavelength at the output center frequency. With output taps at the center of the silicon strip, a total EM phase distortion of nearly 90° results. Amplitude distortion due to EM reflections at the ends of the silicon are eliminated by terminating with chip resistors [19]. Termination with inductors [20] will reduce phase distortion and increase device efficiency, but at the expense of reintroducing amplitude distortion. Another approach to reducing the EM phase distortion is to increase the number of silicon segments and combine the individual outputs with an array of sum–difference hybrids. For example, the last device listed in Table II has four silicon segments. By combining the outputs with three sum–difference hybrids a single output with a total EM phase distortion of 45° is obtained. Other techniques which may be employed include multiple taps on a single convolver output plate and compensation by offsetting the reference center frequency relative to the signal center frequency [26]. Clearly there are engineering solutions to the EM phase distortion problem which have not been fully implemented in the current AE convolver design.

The AE convolver has impressive signal processing capability with demonstrated ruggedness, temperature stability, small size and weight, and wide bandwidth. Design criteria exist with which device parameters can be predicted with a high degree of accuracy. Fabrication procedures and assembly techniques exist which result in reproducible device efficiencies to $\pm 1.5$ dB. Yet, peripheral circuits play a key role in achieving the full processing capabilities of the convolver. The role of circuits is described below.

## IV. Convolver Subsystem

The goal of this section is to outline the basic concepts of a convolver subsystem first demonstrated at Lincoln Laboratory. The subsystem is packaged in two electronic modules, a MSK waveform module and a convolver module, each measuring $18 \times 16 \times 1.9$ cm$^2$ and weighing about 0.8 kg. The MSK waveform module, shown schematically in Fig. 11, supplies two time-reversed reference waveforms. Two additional outputs are available for supplying MSK waveforms to the transmitter during the transmit mode of radio operation. The waveform module generates a spread-spectrum signal with a bit duration of 10.8 $\mu$s and a 92.5-M-chip/s encoding rate. Each bit contains 1024 chips. The impulses which drive the MSK SAW modulator are generated by high-speed emitter-coupled logic (ECL). Considerable amplification ($\sim$50 dB) is required after the MSK SAW modulator to raise the reference signals to the desired 20-dBm power level.

The convolver module, shown schematically in Fig. 12, contains two DPSK convolvers having input bandwidths of

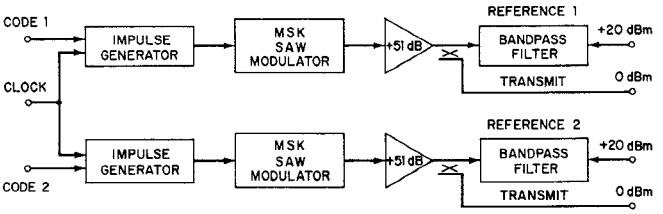


Fig. 11. Schematic of the MSK waveform module.

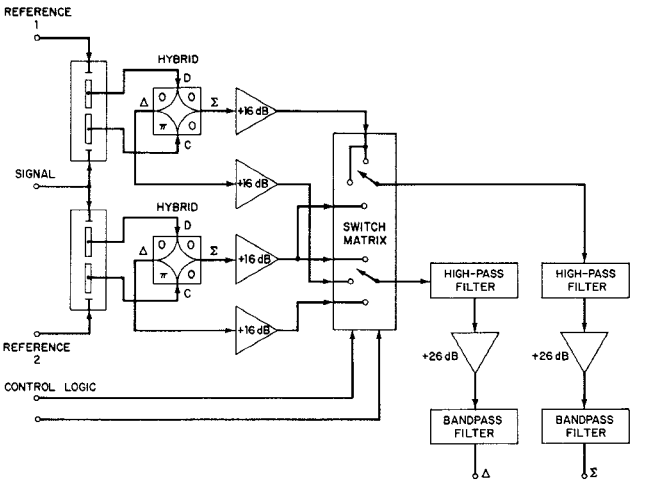


Fig. 12. Schematic of the convolver module.

100 MHz and center frequencies of 300 MHz, sum–difference hybrids, output amplifiers, a switch matrix, and bandpass filters.

The measured dynamic range of the convolver subsystem is 50 dB. This is about 7 dB less than the device dynamic range specified in Table III. The degradation is due to losses in the sum–difference hybrid, a 3.5-dB noise figure for the output amplifiers and spurious signals associated with the reference waveform. The switch matrix in the convolver module allows for convenient selection of the desired outputs from the sum–difference hybrids. The bandpass filters suppress most transient signals associated with the switch matrix.

Matched filters are employed to enhance the signal-to-noise ratio relative to undesirable signals, which in practical situations might include interference due to transmissions which occupy the same spectrum as the signal, intentional jamming of the signal, multipath signals, and receiver front-end noise. The optimum linear filter realization depends on the nature of the desirable and undesirable signals. Therefore, it is not possible to define a single filter which is optimum for a large variety of circumstances. We have elected to measure convolver performance relative to white Gaussian noise at the input of the device, partly because noise sources of this type are available in most laboratories and partly because the results can be compared to expected matched filter results. The user of the device is cautioned to be aware of the limitations of this measurement relative to real situations in which the device is to be employed.

The difference between the ideal and measured output signal-to-noise ratio contributes to the system implementa-

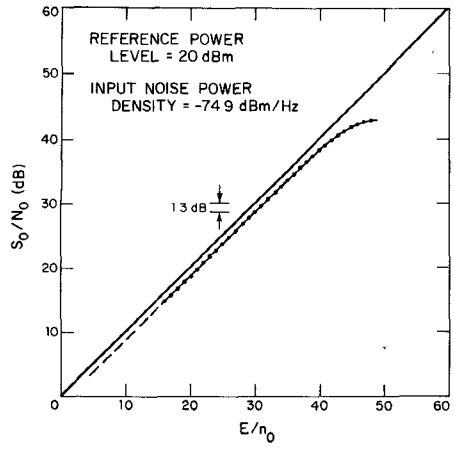


Fig. 13. Convolver performance in the presence of white Gaussian noise.

tion loss. Practically, it is difficult in filters matched to complex signals to measure this loss directly. We have employed an equivalent method [27] by which it is possible to define the loss as

$$L_i = 10\log(2E/n_0) - 10\log(S_o/N_o)\,\text{dB} \qquad (5)$$

where $S_o$ is the measured peak power level of the autocorrelation signal at output, $N_o$ is the measured output noise power due only to input noise, $E$ is the input signal energy in one bit, and $n_0$ is the uniform input noise density over the passband of the device. The relationship given by (5) is based on the fact that the *ideal* peak signal-to-noise ratio at the output is equal to $2E/n_0$.

Because it was difficult to accurately determine the output signal-to-noise ratio with both signal and noise present at the convolver input, the measurements were made separately. The autocorrelation peak power $S_o$ was determined by noting the peak amplitude of the correlation impulse on a high-frequency oscilloscope and then matching that amplitude with a CW signal which was at the same center frequency (600 MHz). The average CW signal power (now equal to half the peak power of $S_o$) and noise output power $N_o$ were measured with a power meter. Since $N_o$ is defined as that portion of the output noise which is due only to white noise entered at the input, care was taken to subtract other noise contributions at the output.

The measurements indicated subsystem implementation losses which ranged from 1 to 2 dB. The results for one device are shown in Fig. 13. The rms value of the sum of the squares of the measurement inaccuracies was 0.7 dB. The phase distortions in the MSK waveform used in the measurements were unknown, but amplitude distortions as high as 30 percent were observed. These distortions may have contributed significantly to the measured implementation loss.

## V. Device Projections

While current convolvers provide impressive signal processing performance, it is worthwhile to project the limits to which device performance can be extended. In considering the limitations in device performance, two figures of merit will be emphasized: 1) processing gain, which is ideally equal to the time-bandwidth product; and 2) dynamic range, which is the difference between the maximum output power and the thermal noise floor (or the maximum spurious level). These two figures of merit are usually sufficient for determining system applicability.

In designing convolvers there are clear tradeoffs between the fractional bandwidth, center frequency and interaction length. For example, the insertion loss of a $LiBnO_3$ delay line increases by 12 dB as the fractional bandwidth is increased from 22 to 44 percent. For AE convolvers the internal efficiency factor $M$ is inversely proportional to both the acoustic frequency and interaction length. A significant loss in the output circuit can occur when the electromagnetic length of the silicon is greater than one-quarter wavelength at the output frequency. These and other tradeoffs constrain the operating range of convolvers. A very important limit is the power input to the device.

Power levels in the AE convolver are limited by two mechanisms: 1) acoustic saturation of the delay line; and 2) saturation of the nonlinear mixing interaction in the semiconductor. Experimental observations indicate that both saturation mechanisms have the same approximate frequency dependence ($\sim 1/f^2$). For devices having moderate interaction lengths (where acoustic propagation losses are under several decibels) the limiting factor in device output power is the saturation of the nonlinear interaction in the silicon. For devices having relatively long processing times, where acoustic propagation losses can be significant, the maximum output power is often limited by acoustic saturation of the SAW delay line. As shown in Table II measured data on the saturation level is available for convolvers having center frequencies up to 500 MHz. The maximum output power is specified at the $F$-factor 1-dB compression point. For center frequencies above 500 MHz, extrapolation of the saturation level was made from experimental data.

For both acoustic and silicon saturation [10], [19] the degradation in $F$-factor is relatively gradual. While employing pseudonoise input signals having about 1000 chips per bit, several devices were driven about 5 dB beyond their 1-dB compression points. No degradation in the peak-to-sidelobe levels were observed. This indicates that the devices can be driven moderately beyond their saturation points without any significant degradation in system performance.

The dynamic range of the convolver must support its available processing gain [28]. Consider the worst-case interference condition. The jamming power is at the maximum device input level, while the input signal is below the jammer by a ratio equal to the processing gain less the minimum useful signal-to-noise ratio. In an ideal device, the input interference which appears at the device output is reduced by the processing gain. However, for a device with finite dynamic range, the thermal noise floor due to the output amplifier (or the inherent device spurious level) adds to the noise component at the device output. This results in a noise level which would be produced by an ideal device with less processing gain. If the noise floor is 10 dB below the interference level, a degradation of 0.4 dB occurs. Thus the convolver must have a dynamic range

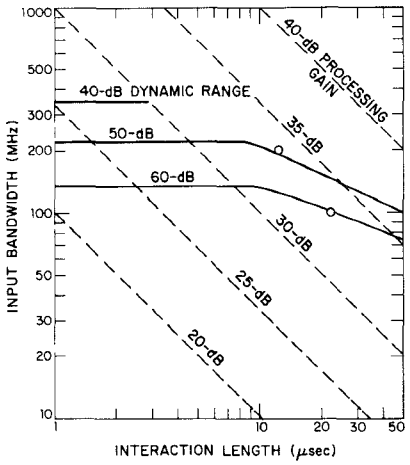


Fig. 14. Time-bandwidth plot projecting the limitations of dynamic range (solid lines) and processing gain (dashed lines) for gap-coupled AE convolvers. The experimental points (circles) represent the 100- and 200-MHz bandwidth convolvers.

which is approximately 10 dB larger than its processing gain. For this reason, the projections are limited to devices which have dynamic ranges which are at least 10 times the processing gain.

The limits of applicability of AE convolvers to systems can be projected with the aid of Fig. 14, in which the loci of constant processing gain and dynamic range are shown on in time-bandwidth space. In the projections, maximum fractional bandwidths of 45 percent or less were assumed for the $LiNbO_3$ delay lines. Processing times were limited to 50 $\mu$s which is consistent with $LiNbO_3$ substrates having a maximum length of 20 cm. Also included on this plot are experimental points for the DPSK convolvers discussed in Section II. It is seen from this figure that the maximum performance likely to be achieved via the AE convolver technology is 37-dB processing gain with 47-dB dynamic range.

## VI. Summary

Convolver input bandwidths of 200 MHz and processing gains of 33 dB with adequate dynamic range are available in well-engineered acoustoelectric devices. These convolvers possess mechanical ruggedness as well as temperature stability. They offer processing gains within 1 dB of that theoretically possible. Thus acoustoelectric convolvers have clearly reached a development level at which they are ready for field deployment in advanced spread-spectrum communications equipment.

Basic systems concepts in the implementation of acoustoelectric convolvers originated at Lincoln Laboratory. Both device and system technology have been transferred by Lincoln Laboratory to industry. The systems engineer is now challenged to find unique ways to deploy the convolver, to develop new system concepts which exploit the full potential of the convolver, and to upgrade and integrate peripheral circuits, especially the digital code generators, in order to reduce size and power consumption.

## Acknowledgment

The author is pleased to acknowledge W. M. Brown and J. H. Cafarella for the circuit and system concepts, J. H. Cafarella, J. H. Goll, and I. Yao for their multiple contributions to convolver technology and development and E. Stern and R. W. Ralston for their guidance and consultation. The extensive work by R. P. Baker on the electronics modules, R. L. Slattery and W. Brogan on device fabrication, and I. M. Coates and P. R. Phinney in the gap assembly is also gratefully acknowledged.

## References

[1] J. H. Cafarella, W. M. Brown, E. Stern, and J. A. Alusow, "Acoustoelectric convolvers for programmable matched filtering in spread spectrum systems," *Proc. IEEE*, vol. 64, pp. 756–759, May 1976.

[2] S. A. Reible, J. H. Cafarella, R. W. Ralston, and E. Stern, "Convolvers for DPSK demodulation of spread spectrum signals," in *1976 IEEE Proc. Ultrasonics Symp.*, pp. 451–455.

[3] D. C. Malocha, J. H. Goll, and M. A. Heard, "Design of a compensated SAW filter used in a wide spread MSK waveform generator," in *1979 IEEE Proc. Ultrasonics Symp.*, pp. 518–521.

[4] D. Brodtkorb and J. E. Laynor, "Fast synchronization in a spread spectrum system based on acoustoelectric convolvers," in *1978 IEEE Proc. Ultrasonics Symp.*, pp. 561–566.

[5] W. C. Wang, "Signal generation via nonlinear interaction of oppositely directed sonic waves in piezo-electric semiconductors," *Appl. Phys. Lett.*, vol. 18, pp. 337–338, Apr. 1971.

[6] W. L. Bongianni, "Pulse compression using nonlinear interaction in surface acoustic wave convolver," *Proc. IEEE*, vol. 59, pp. 713–714, Apr. 1971.

[7] W. D. Damon, W. T. Meloney, and D. H. McMahon, "Interaction of light with ultrasound: Phenomena and applications," in *Physical Acoustics*, vol. VII, New York: Academic, 1970.

[8] G. S. Kino, "Zinc oxide on silicon acoustoelectric devices," in *1979 IEEE Proc. Ultrasonics Symp.*, pp. 900–910.

[9] J. H. Goll and N. J. Tolar, "Improved efficiency of high BT product SAW convolvers," in *1977 IEEE Proc. Ultrasonics Symp.*, pp. 469–471.

[10] I. Yao and S. A. Reible, "Wide bandwidth acoustoelectric convolvers," in *1979 IEEE Proc. Ultrasonics Symp.*, pp. 701–705.

[11] S. A. Reible, K. L. Wang, and V. S. Dolat, "Transverse modes in acoustoelectric convolvers," in *1978 IEEE Proc. Ultrasonics Symp.*, pp. 48–53.

[12] P. H. Defranould and C. Maerfeld, "Acoustic convolver using multistrip beamwidth compressors," in *1974 IEEE Proc. Ultrasonics Symp.*, pp. 224–227.

[13] R. A. Becker and D H. Hurlburt, "Wideband $LiNbO_3$ elastic convolver with parabolic horns," in *1979 IEEE Proc. Ultrasonics Symp.*, pp. 729–731.

[14] I. Yao, "High performance elastic convolver with parabolic horns," in *1980 IEEE Proc. Ultrasonic Symp.*, to be published.

[15] R. A. Becker, S. A. Reible, and R. W. Ralston, "Comparison of acoustoelectric and acoustooptic signal processing devices," in *Optical Signal Processing for C³I*, Bellingham, WA: SPIE, 1979, pp. 126–133.

[16] R. E. Kahn, S. A. Gronemeyer, J. Burchfiel, and R. C. Kunzelman, "Advances in packet radio technology," *Proc. IEEE*, vol. 66, pp. 1468–1496, Nov. 1978.

[17] W. Smith, "SAW filters for CPSM spread spectrum communications," in *1977 IEEE Proc. Ultrasonics Symp.*, pp. 524–528.

[18] J. H. Goll and D. C. Malocha, "High bandwidth spread spectrum communications using SAW convolvers," *Microwave Theory Tech.*, pp. 000–000, this issue.

[19] J. H. Cafarella, J. A. Alusow, W. M. Brown, and E. Stern, "Programmable matched filtering with acoustoelectric convolvers in spread-spectrum systems," in *1975 IEEE Proc. Ultrasonics Symp.*, pp. 205–208.

[20] J. H. Goll and R. C. Bennett, "Reactive output tuning of high BT product SAW convolvers," in *1978 IEEE Proc. Ultrasonics Symp.*, pp. 44–47.

[21] F. J. Leonberger, R. W. Ralston, and S. A. Reible, "Gap-coupled

$InSb/LiNbO_3$ acoustoelectric convolver operating at 77 K," *Appl. Phys. Lett.*, vol. 33, pp. 484–486, Sept. 1978.
[22] J. H. Cafarella, private communication.
[23] T. M. Reeder, W. S. Shreve, and P. L. Adams, "A new broadband coupling network for interdigital surface wave transducers," *IEEE Trans. Sonics Ultrason.*, vol. SU-19, pp. 466–477, Oct. 1972.
[24] I. Yao, private communication.
[25] J. H. Holtham and R. C. Williamson, "Automatic pulsed technique for measuring phase and amplitude response of SAW devices," in *1978 IEEE Proc. Ultrasonics Symp.*, pp. 607–610.
[26] E. L. Adler, "Electromagnetic Long-Line Effects In SAW Convolvers," in *1980 IEEE Proc. Ultrasonics Symp.*, to be published.
[27] See, for example, M. Schwartz, W. R. Bennett, and S. Stein, *Communication Systems and Techniques*. New York: McGraw-Hill, 1966, p. 67.
[28] J. H. Cafarella, "Device requirements for spread-spectrum communication," in *Optical Signal Processing for $C^3I$*, Bellingham, WA: SPIE, 1979, vol. 209, pp. 53–56.

# An Application of SAW Convolvers to High Bandwidth Spread Spectrum Communications

JEFFREY H. GOLL, MEMBER, IEEE, AND DONALD C. MALOCHA, MEMBER, IEEE

*Abstract*—**A spread spectrum communications subsystem that is based on the separated medium acoustoelectric convolver is described. The subsystem generates minimum-shift-keyed (MSK) waveforms with the aid of SAW filters and performs differential-phase-shift-keyed (DPSK) data demodulation with acoustoelectric convolvers. The convolver provides a *BT* product of 2200 with a 3-dB bandwidth of 100 MHz. The signals processed by the subsystem have a *BT* product of 1100. In this paper, the subsystem, the generation of MSK waveforms, and the use of acoustoelectric convolvers are described. Important subsystem performance characteristics, including dynamic range ($\simeq$50 dB), contribution to implementation loss ($\simeq$1 dB), DPSK demodulation, and distortion levels are illustrated and discussed.**

## I. Introduction

THE ACOUSTOELECTRIC convolver [1], [2] is a programmable matched filter with a unique combination of demonstrated large processing gain, good dynamic range, broad bandwidth, small size and weight, and low drive power requirements. It provides the central component for a high data rate spread spectrum communications receiver. A convolver-based system can provide secure spread spectrum communications [3] with fast synchronization [4], low probability of intercept transmission, and good jammer immunity. In contrast with conventional matched filters based on surface acoustic wave (SAW) tapped delay lines, the convolver processing gain is virtually independent of temperature. Decoding of differential-phase-shift-keyed (DPSK) data can be conveniently accomplished with a dual convolver [5]. Wide-band minimum-phase-shift-keyed (MSK) waveforms for use with the convolver can be generated with the aid of an appropriately designed SAW filter [6].

Highly developed gap-coupled acoustoelectric convolvers [5], [7]–[9] provide processing gains of up to 33 dB with adequate dynamic range and input bandwidths of 100 MHz. Recently, an acoustoelectric convolver with an input bandwidth of 200 MHz has been demonstrated [10]. The mechanical support structure of the device insures stable operation over a 100°C temperature range [5], [10]. Such devices have passed stringent vibration tests for military

Manuscript received April 24, 1980; revised September 22, 1980. This work was supported by the Defense Advanced Research Projects Agency and the Department of the Army.

J. H. Goll is with the Central Research Laboratories, Texas Instruments Inc., Dallas, TX 75265.

D. C. Malocha was with the Central Research Laboratories, Texas Instruments Inc., Dallas, TX. He is now with Sawtek Inc., Orlando, FL 32854.

0018-9480/81/0500-0473$00.75 ©1981 IEEE